MAST: A Quickest Detection Procedure for COVID-19 Epidemiological Data to Trigger Strategic Decisions

Paolo Braca
Research Department
NATO STO CMRE
La Spezia, 19126, Italy
paolo.braca@cmre.nato.int

Domenico Gaglione
Research Department
NATO STO CMRE
La Spezia, 19126, Italy
domenico.gaglione@cmre.nato.int

Stefano Marano
DIEM
University of Salerno
Fisciano (SA), 84084, Italy
marano@unisa.it

Leonardo M. Millefiori
Research Department
NATO STO CMRE
La Spezia, 19126, Italy
leonardo.millefiori@cmre.nato.int

Peter Willett
ECE Department
University of Connecticut
Storrs (CT), 06269, USA
peter.willett@uconn.edu

Krishna Pattipati
ECE Department
University of Connecticut
Storrs (CT), 06269, USA
krishna.pattipati@uconn.edu

***Abstract*—Signal processing tools play an important role in interpreting COVID-19 pandemic data, and thence contribute to timely and rational decisions. We recently proposed a sequential test (MAST) designed to detect the passage from a controlled to a critical regime of the COVID-19 pandemic; and similarly from critical to controlled. In this paper we provide a performance assessment and analysis of MAST alerts from official COVID-19 infection data–the number of daily new positives and hospitalized individuals in several Italian regions.**

***Index Terms*—COVID-19 pandemic, quickest detection, MAST, pandemic waves.**

I. Introduction

The virus known as SARS-CoV-2 (severe acute respiratory syndrome coronavirus 2) is the cause of the respiratory illness responsible for the COVID-19 pandemic. It has changed our lives and is expected to have a profound long-term impact worldwide. Containment of the spread of COVID-19 relied mainly on confinement measures aimed at "flattening the curve" of infections to avoid overwhelming the healthcare systems. These measures ranged from travel and social gathering restrictions to closures of a significant portion of commercial activities. Though these measures helped control the spread of COVID-19, they also created unprecedented economic crises and caused significant social unrest [1].

The effects stemming from the imposition of restrictive measures demonstrate the importance of making timely and rational decisions. Recent studies aimed at providing rigorous methodological support to these decisions involve many different scientific fields [2]–[5], and in particular by signal processing tools, see e.g., [6], [7].

In [8], we proposed a variation of the celebrated Page's test, called MAST (mean-agnostic sequential test), which is designed to detect the transition from a *controlled regime*, where the spreading of COVID-19 is limited, to a *critical regime*, in which the infection spreads exponentially fast. In [9], we provided a first analysis of MAST on the sequences of daily new positive individuals from 14 different countries. In [10], we integrated MAST within a detection-estimation-forecasting framework designed to: (i) learn relevant features of the epidemic (e.g., the infection rate); (ii) detect as quickly as possible the onset (or the termination) of an exponential growth of the contagion; (iii) reliably forecast the epidemic's evolution [11].

In this work, we consider two COVID-19 time series: the number of daily new positive individuals, and the current number of hospitalized individuals. Leveraging the inherent multiplicative nature of the pandemic evolution, we analyze the ratio of successive samples of the time series, defined as follows. For $k = 1, 2, \dots,$ denoting the day index:

$$\begin{cases} x_k = \dfrac{p_{k+1}}{p_k}, & \text{with } p_k \text{ the daily new positive cases,} \\ y_k = \dfrac{h_{k+1}}{h_k}, & \text{with } h_k \text{ the hospitalized individuals.} \end{cases} \tag{1}$$

We shall assume that the sequences $\{x_k\}_{k=1}^n$ and $\{y_k\}_{k=1}^n$ are made of conditionally independent samples. To the best of our knowledge, this is the first study of COVID-19 infection time series that is based on the ratios of successive time samples, with the exception of in-progress works by our group [9], [10].

II. Derivation of the MAST

In the following, we derive the structure of the detector used in the analysis with reference to the sequence $\{x_k\}_{k=1}^n$. The

P. Willett was supported by AFOSR under FA9500-18-1-0463 and by NIUVT. The work by K. R. Pattipati was supported in part by the U.S. Office of Naval Research, in part by the U.S. Naval Research Laboratory under grants N00014-18-1-1238 and N00173-16-1-G905, and in part by the Space Technology Research Institutes from NASA's Space Technology Research Grants Program under grant 80NSSC19K1076.

same derivation holds for $\{y_k\}_{k=1}^n$. Let us start by considering two pandemic regimes, say "controlled" and "critical", in which the observations are assumed to be Gaussian distributed $x_k \sim \mathcal{N}(\mu_{i,k}, \sigma)$ with mean values $\mu_{0,k}$ and $\mu_{1,k}$, respectively. The goal is to detect as soon as possible if a change from the controlled to the critical regime is present in the sequence of observations $\{x_k\}_{k=1}^n$. The problem can be cast in a hypothesis testing framework [12], [13]:

$$\begin{aligned} &\text{no change}: \quad x_k \sim \mathcal{N}(\mu_{0,k}, \sigma), \qquad k = 1, \ldots, n, \\ &\text{change}: \quad \begin{cases} x_k \sim \mathcal{N}(\mu_{0,k}, \sigma), & k = 1, \ldots, j-1, \\ x_k \sim \mathcal{N}(\mu_{1,k}, \sigma), & k = j, \ldots, n, \end{cases} \end{aligned} \tag{2}$$

where the observations $\{x_k\}_{k=1}^n$ are independent Gaussian random variables of known variance σ^2. The mean values $\{\mu_{i,k}\}_{k=1}^n$, $i = 0, 1$, are unknown time-varying deterministic parameters, verifying the constraints: for $k = 1, 2, \ldots, n$,

$$\mu_{0,k} \leq 1 \qquad \text{(controlled regime)}, \tag{3a}$$

$$\mu_{1,k} > 1 \qquad \text{(critical regime)}. \tag{3b}$$

Under the "change" hypothesis, the time instant $1 \leq j \leq n+1$ at which the mean value switches from complying with (3a) to complying with (3b), is modeled as an unknown deterministic parameter and defines the onset of a flare-up of the pandemic. Under the "no change" hypothesis, no switch occurs and the switch index j is formally set to $n+1$. Model (2) contains $2n+1$ unknown parameters: the index j and the two sequences of the mean values. The problem formulation fits exactly the classical quickest detection framework, with additional uncertainty represented by the $2n$ unknown mean values. Accordingly, the MAST detector that we are going to derive is a tailored version of the celebrated Page's test, see, e.g., [14], [15].

The generalized likelihood ratio test (GLRT) approach evaluates the likelihood ratio of the two hypotheses by replacing the unknown parameters with their hypothesis-constrained maximum likelihood (ML) estimates [12], [13]. For the decision problem (2), the GLRT statistic takes the expression

$$\frac{\displaystyle\sup_{1 \leq j \leq n+1} \prod_{k=1}^{j-1} \sup_{\mu_{0,k} \leq 1} e^{-\frac{(x_k - \mu_{0,k})^2}{2\sigma^2}} \prod_{k=j}^{n} \sup_{\mu_{1,k} > 1} e^{-\frac{(x_k - \mu_{1,k})^2}{2\sigma^2}}}{\displaystyle\prod_{k=1}^{n} \sup_{\mu_{0,k} \leq 1} e^{-\frac{(x_k - \mu_{0,k})^2}{2\sigma^2}}},$$

which can be cast in a more convenient form after recognizing that the ML estimates of the mean values are

$$\widehat{\mu}_{0,k} = \min(x_k, 1), \tag{4a}$$

$$\widehat{\mu}_{1,k} = \max(x_k, 1), \tag{4b}$$

yielding

$$\max_{1 \leq j \leq n+1} \prod_{j \leq k \leq n \,:\, x_k \leq 1} e^{-\frac{(x_k - 1)^2}{2\sigma^2}} \prod_{j \leq k \leq n \,:\, x_k > 1} e^{\frac{(x_k - 1)^2}{2\sigma^2}}. \tag{5}$$

Taking the logarithm of (5), the GLRT decision rule is equivalent to the following test

$$T_n = \max_{1 \leq j \leq n+1} \sum_{\substack{k=j \\ k:\, x_k > 1}}^{n} \frac{(x_k - 1)^2}{2\sigma^2} - \sum_{\substack{k=j \\ k:\, x_k \leq 1}}^{n} \frac{(x_k - 1)^2}{2\sigma^2} \underset{\text{no change}}{\overset{\text{change}}{\gtrless}} \gamma, \tag{6}$$

and the exponential growth of the pandemic is declared on day n^*, the first occurrence of threshold crossing, that is, $n^* = \min\{n \geq 1 \,:\, T_n > \gamma\}$.

It is not hard to show that MAST (analogous to the classical Page's test) admits a recursive expression, which makes it particularly appealing for practical usage in detecting the pandemic's exponential growth. After some simple algebraic manipulations, one gets: $T_0 = 0$ and, for $n \geq 1$,

$$T_n = \max\left[0, T_{n-1} + \frac{(x_n - 1)^2}{2\sigma^2} \operatorname{sign}(x_n - 1)\right], \tag{7}$$

where $\operatorname{sign}(z) = 1$ for $z > 0$ and $\operatorname{sign}(z) = -1$ otherwise. Furthermore, we note that the MAST statistic in (7) can be formally obtained from the Page's test statistic by replacing in the latter the unknown mean with $|x_n - 1|$; details in [8].

We consider two performance figures for the MAST decision rule:

- the mean delay $\Delta = \mathbb{E}_1\left[\, n^* - j \,\right]$, which is the delay in declaring the pandemic onset under the "change" hypothesis (whence the subscript 1 appended to the expectation), where j is the true onset of change and n^* is when the onset is declared;
- the risk R, which is the reciprocal of the mean time between two threshold crossings under the "no change" hypothesis, assuming that, at each crossing, the MAST decision statistic is reset to zero.

We recall from [8], [9] that the mean delay Δ varies almost linearly with the threshold, i.e., $\Delta \propto \gamma$, whereas the logarithm of the risk $\log R$ varies almost linearly with the opposite of the threshold, i.e., $\log R \propto -\gamma$.

It is clear that the previous derivations and definitions can be repeated *mutatis mutandis* to detect the passage from (3b) to (3a), rather than from (3a) to (3b), by defining the "change" hypothesis in (2) as follows:

$$\text{change}: \quad \begin{cases} x_k \sim \mathcal{N}(\mu_{1,k}, \sigma), & k = 1, \ldots, j-1, \\ x_k \sim \mathcal{N}(\mu_{0,k}, \sigma), & k = j, \ldots, n. \end{cases} \tag{8}$$

The details are omitted and the final result is the "reversed MAST," whose iterative form is: $\bar{T}_0 = 0$ and, for $n \geq 1$,

$$\bar{T}_n = \max\left[0, \bar{T}_{n-1} + \frac{(x_n - 1)^2}{2\sigma^2} \operatorname{sign}(1 - x_n)\right]. \tag{9}$$

III. Results

A preliminary performance evaluation of the proposed test and a comparison with the classical Page's test are provided in [8]. Here, we apply the MAST procedure and evaluate its performance on official COVID-19 data in Italy. Specifically, we use the sequences of daily new positive individuals and hospitalized individuals provided, for each Italian region, by the Italian Civil Protection Department (CPD) [16].

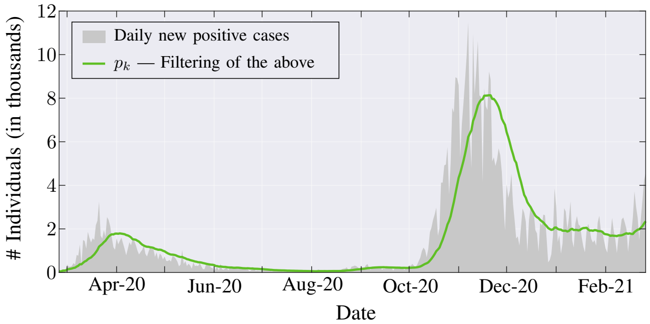

(a) Daily new positive cases.

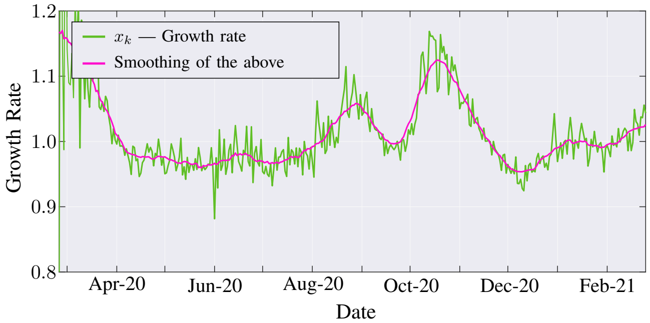

(b) Growth rate.

Fig. 1. (a) Daily new positive individuals in Lombardia region, Italy, since February 25, 2020, and its averaged version obtained with a 21-days causal MA filter with uniform weigths (green line). (b) Growth rate of the epidemic computed from the averaged daily new positive cases (green line); for easier visualization, we also show its smoothed version obtained through a non-causal MA filter with uniform weights of length 21 days (magenta line).

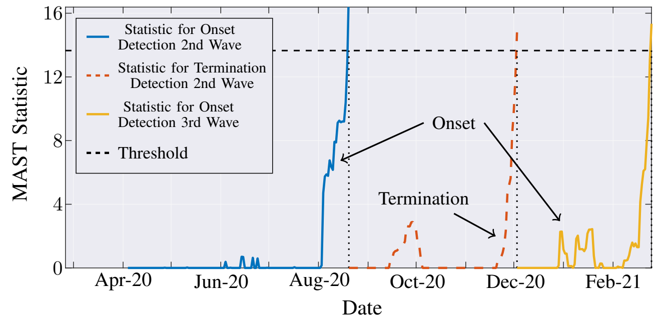

Fig. 2. Analysis for the Lombardia region using the sequence of daily new positive individuals. We show the MAST statistics T_n and $\bar{T}_n$ computed, starting from April 4, 2020, for the onset detection of the second wave (blue solid line) and the third wave (yellow solid line), and for the termination detection of the second wave (red dashed line). The threshold (black dashed line) corresponds to the risk $R = 10^{-5}$ days^{-1}. The onset and termination of the second wave are declared on August 20, and December 3, 2020, respectively. The onset of the third wave is declared on February 25, 2021.

A. Time Series Processing

The time series processing is described with reference to the sequence of daily new positive cases. The same procedure is also applied to the sequence of hospitalized individuals, with an important difference that will be mentioned soon.

Figure 1a shows an illustrative sequence, in grey, of daily new positive cases in the Lombardia region, Italy, from the end of February, 2020, to the end of February, 2021. These data present gross errors due, e.g., to missing values and delays in information reporting, as well as weekly oscillations. For instance, it is seen that the number of reported cases over the weekend is systematically smaller than the values recorded on weekdays. To address these issues, the sequence of daily new positive cases is smoothed by a 21-day causal moving average (MA) filter with uniform weights. The smoothed sequence, shown in green in Fig. 1a, represents the time series $\{p_k\}_{k=1}^n$ in (1). The delay effect of the causal filtering operation is evident. The sequence of hospitalized individuals is less affected by gross errors and weekly oscillations and therefore it does not require the smoothing operation.

The ratio of successive samples of (filtered) daily new positive individuals, referred to as $\{x_k\}_{k=1}^n$ in (1) — used to compute the MAST statistics T_n in (7) and $\bar{T}_n$ in (9) — is shown in green in Fig. 1b. As mentioned in Section II, each element x_k of the sequence of observations is modeled as an independent Gaussian random variable with known variance σ^2 and unknown mean value. Actually, the variance is not known *a priori* but is estimated from the data, using the smoothed version of the growth rate sequence $\{x_k\}_{k=1}^n$, shown in Fig. 1b by the magenta curve. In practical cases, the variance should be obtained by other means. Regarding the Gaussian assumption, Kolmogorov-Smirnov goodness-of-fit tests pass at 5% significance level in almost all cases for reasonably rich data intervals of 60 days. This is so for sequences both of daily new positive and hospitalized individuals, with sole exceptions of Calabria and Sardegna, respectively. Over larger intervals, the validity of the Gaussian assumption is less clear, presumably because of a slowly changing variance.

B. Results for the Lombardia Region

For the Lombardia region, Fig. 2 depicts the MAST statistics T_n and $\bar{T}_n$. The former is used to detect the onset of the second and third epidemic waves, and the latter to detect the termination of the second wave. The value of the threshold γ corresponds to the risk $R = 10^{-5}$ days^{-1}, which means that a false change of regime is declared, on average, every 270 years.

The statistic T_n is represented by the blue solid line; its recursive computation starts on April 4, 2020. The onset of the second wave is declared on August 20, 2020. On this day, the statistic $\bar{T}_n$ used to detect the termination of the second wave is initiated, and its evolution is reported in dashed red; the termination of the second wave is detected on December 3, 2020. Finally, the yellow solid line represents the statistic T_n initiated on December 3, 2020, used for the detection of the third wave, which is detected on February 25, 2020. The same analysis is carried for the province of Brescia (smaller area in Lombardia). From Fig. 3, we observe that this province is impacted by a total of four waves and the most recent one is declared on February 10, 2021, that is, 15 days earlier than the detection at regional level. This result demonstrates the capability of the MAST to be used at different levels of granularity, thus allowing the authorities to intervene on small clusters of the population to contain the contagion.

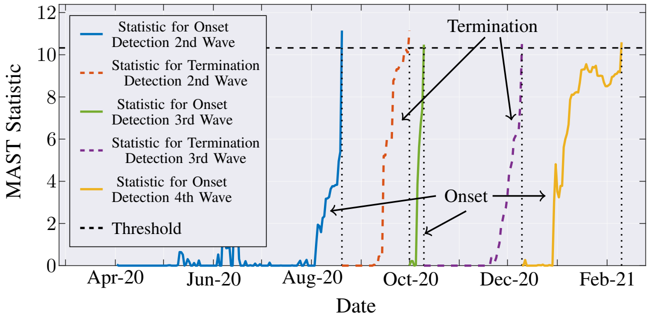

Fig. 3. Analysis for the province of Brescia, using the sequence of daily new positive individuals. We show the MAST statistics T_n and $\bar{T}_n$ computed, starting from April 2, 2020, for the onset detection of the second wave (blue solid line), the third wave (green solid line), and the fourth wave (yellow solid line), and for the termination detection of the second wave (red dashed line) and the third wave (purple dashed line). The threshold (black dashed line) corresponds to risk $R = 10^{-5}$ days^{-1}. The most recent wave is declared on February 10, 2021.

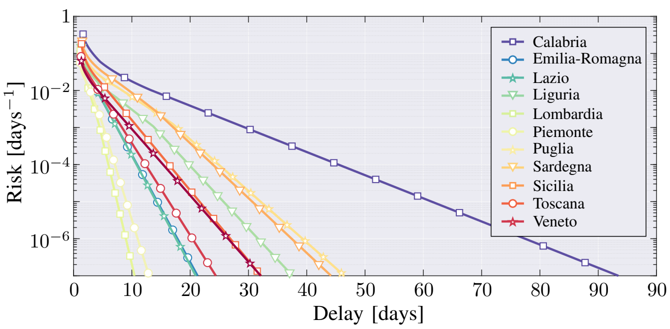

(a) Sequence of daily new positive individuals.

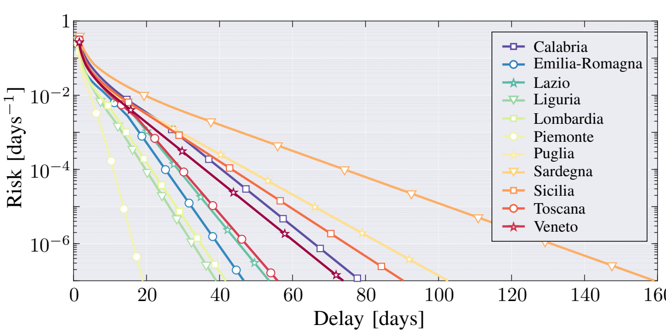

(b) Sequence of hospitalized individuals.

Fig. 4. MAST performance in terms of risk R versus mean delay Δ, computed for 11 Italian regions using (a) the sequence of daily new positive individuals $\{p_k\}$, and (b) the sequence of hospitalized individuals $\{h_k\}$.

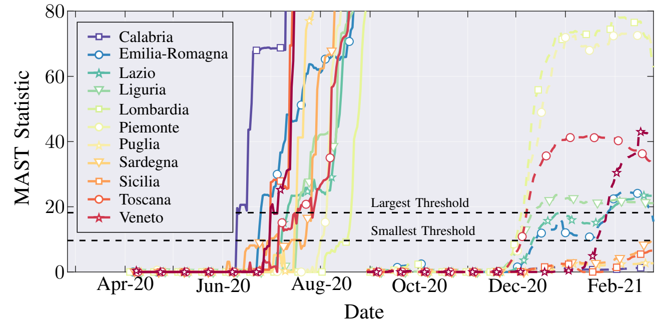

(a) Sequence of daily new positive individuals.

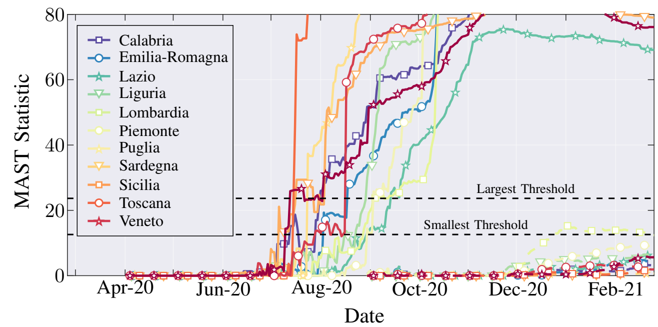

(b) Sequence of hospitalized individuals.

Fig. 5. MAST statistics T_n (solid lines) and $\bar{T}_n$ (dashed lines) computed for 11 Italian regions using (a) the sequence of daily new positive individuals p_k, and (b) the sequence of hospitalized individuals h_k. The statistics are employed to detect the onset (T_n) and termination ($\bar{T}_n$) of the COVID-19 second wave. The dashed horizontal lines represent the smallest and largest thresholds corresponding to $R = 10^{-5}$ days^{-1} for the ensemble of the 11 regions. Curves are prolonged beyond threshold crossing for clarity.

C. Results for 11 Italian Regions

In this subsection, we analyze the performance and behavior of MAST using the sequences of daily new positive cases and hospitalized individuals from 11 Italian regions.

A comparison of the performance in terms of risk R versus mean delay Δ is addressed in Fig. 4a for the sequence of daily new positive cases, and in Fig. 4b for the sequence of hospitalized individuals. Though the implementation of MAST does not require knowledge of the mean sequences $\{\mu_{0,k}\}_{k=1}^n$ and $\{\mu_{1,k}\}_{k=1}^n$, the assessment of its performance depends on the specific scenario, and thus on the mean sequences of the region under consideration. In addition, for performance assessment, arbitrarily long mean sequences are in principle required. Therefore, for each Italian region, periodic counterparts of the estimated mean sequences $\{\widehat{\mu}_{0,k}\}_{k=1}^n$ and $\{\widehat{\mu}_{1,k}\}_{k=1}^n$ are constructed and used to obtain the relationships between Δ and γ, and between R and γ, for small values of the threshold γ. This is achieved by standard Monte Carlo computer experiments, involving $5 \cdot 10^4$ independent runs for each value of the threshold γ. Then, since the relation between Δ and γ is almost exactly linear, and the relation between R and γ is almost exactly exponential, values of the mean delay Δ and risk R are extrapolated for arbitrarily large values of the threshold, providing the curves in Fig. 4a and Fig. 4b. Further details on the MAST performance evaluation procedure are in [9].

We observe that, accepting the risk $R = 10^{-5}$ days^{-1}, the mean delay Δ is approximately 7 days for Lombardia and 32 days for Puglia, when using the sequence of daily new positive cases, and below 14 days for Piemonte and approximately 66 days for Puglia, when using the sequence of hospitalized individuals. Overall, given a specific risk level, the mean delay is higher with the sequence of hospitalized individuals. As intuition suggests, during an outbreak, the number of daily new positive cases increases more quickly than the number of hospitalized individuals, hence leading to a quicker detection.

Figures 5a and 5b show the statistics T_n (solid lines) and $\bar{T}_n$ (dashed lines) computed for the 11 Italian regions under

TABLE I
DAY OF DETECTION OF THE ONSET OF THE SECOND WAVE USING THE SEQUENCE OF DAILY NEW POSITIVE CASES

REGION	$R = 10^{-4}$	$R = 10^{-5}$	$R = 10^{-6}$
Calabria	June 10	June 10	June 17
Emilia Romagna	June 23	June 24	June 24
Lazio	July 8	July 8	July 9
Liguria	July 18	July 18	July 20
Lombardia	August 18	August 20	August 20
Piemonte	August 1	August 4	August 5
Puglia	July 16	July 17	July 18
Sardegna	July 24	July 24	July 27
Sicilia	July 1	July 1	July 1
Toscana	July 6	July 6	July 7
Veneto	June 29	July 1	July 1

TABLE II
DAY OF DETECTION OF THE ONSET OF THE SECOND WAVE WITH $R = 10^{-5}$

REGION	DAILY NEW POSITIVE CASES	HOSPITALIZED
Calabria	June 10	July 31
Emilia Romagna	June 24	August 3
Lazio	July 8	September 11
Liguria	July 18	August 30
Lombardia	August 20	September 2
Piemonte	August 4	August 30
Puglia	July 17	July 24
Sardegna	July 24	July 17
Sicilia	July 1	July 15
Toscana	July 6	August 17
Veneto	July 1	July 10

consideration using the sequence of daily new positive cases and the sequence of hospitalized individuals, respectively. In both cases, T_n is initiated when the first wave vanishes and is used to detect the onset of the second wave; $\bar{T}_n$ is initiated on September 1, 2020, and is used to detect the termination of the second wave. Since the threshold, for a given risk level, is region-dependent, the smallest and largest thresholds corresponding to the risk $R = 10^{-5}$ days^{-1} are shown.

From Fig. 5a, we observe that, when using the sequence of daily new positive cases, the onset of the second wave is declared for all the regions between June 10, and August 20, 2020. The day of detection, for each region and for three risk levels, is provided in Table I. These results emphasize the robustness of the MAST detector. Indeed, reducing the risk by a factor 10 or 100, comes at the cost of detection delays of a few days.

The termination of the second wave is detected only for 7 of the 11 regions. The earliest detection is for Lombardia on December 3, 2020, and the latest is for Veneto on January 21, 2021. As for Calabria, Puglia, Sardegna and Sicilia, the statistic $\bar{T}_n$ does not cross the threshold; the second wave in these regions is still ongoing on February 25, 2021.

When using the sequence of hospitalized individuals, we note from Fig. 5b that the detection of the onset of the second wave is, as expected, delayed for most of the regions, except that for Sardegna. A comparison with the detection obtained with the sequence of daily new positive cases is provided in Table II, from which we note that the delay— excluding Sardegna—is of about 31 days. Finally, the termination of the second wave is not detected for any of the regions.

IV. CONCLUSIONS

A sequential test, termed MAST, has been recently proposed in [8]. It was designed to detect the transition from a controlled regime, in which the spread of COVID-19 is limited, to a critical regime, in which the infection spreads exponentially fast. Here, we provided a performance assessment and a behavior analysis of MAST when applied to two different time series of contagion data from several Italian regions: daily new positive cases and hospitalized individuals. We observed that when using the sequence of daily new positive cases, MAST detects the onset of uncontrolled growth with a mean delay of a few days at relatively low risk levels. As expected, the detection is delayed when using the sequence of hospitalized individuals: this can be explained because, during an outbreak, the number of hospitalized individuals increases more slowly than the number of daily new positive cases.

REFERENCES

[1] L. M. Millefiori, P. Braca, D. Zissis, G. Spiliopoulos, S. Marano, P. K. Willett, and S. Carniel, "COVID-19 impact on global maritime mobility," 2021, (under review). [Online]. Available: https://arxiv.org/abs/2009.06960

[2] R. M. Anderson, H. Heesterbeek, D. Klinkenberg, and T. D. Hollingsworth, "How will country-based mitigation measures influence the course of the COVID-19 epidemic?" *Lancet*, vol. 395, no. 10228, pp. 931–934, Mar. 2020.

[3] J. Hellewell, S. Abbott, A. Gimma, N. I. Bosse *et al.*, "Feasibility of controlling COVID-19 outbreaks by isolation of cases and contacts," *Lancet Glob. Health*, vol. 8, no. 4, pp. e488–e496, Apr. 2020.

[4] B. F. Maier and D. Brockmann, "Effective containment explains subexponential growth in recent confirmed COVID-19 cases in China," *Science*, vol. 368, no. 6492, pp. 742–746, May 2020.

[5] J. Dehning, J. Zierenberg, F. P. Spitzner, M. Wibral, J. P. Neto, M. Wilczek, and V. Priesemann, "Inferring change points in the spread of COVID-19 reveals the effectiveness of interventions," *Science*, vol. 369, no. 6500, Jul. 2020.

[6] R. Eletreby, Y. Zhuang, K. M. Carley, O. Yağan, and H. V. Poor, "The effects of evolutionary adaptations on spreading processes in complex networks," *PNAS*, vol. 117, no. 11, pp. 5664–5670, Mar. 2020.

[7] S. Marano and A. H. Sayed, "Decision-making algorithms for learning and adaptation with application to COVID-19 data," May 2021, (under review). [Online]. Available: https://arxiv.org/abs/2012.07844

[8] P. Braca, D. Gaglione, S. Marano, L. M. Millefiori, P. Willett, and K. Pattipati, "Quickest detection of COVID-19 pandemic onset," *IEEE Signal Process. Lett.*, vol. 28, pp. 683–687, Mar. 2021.

[9] ——, "Decision support for the quickest detection of critical COVID-19 phases," *Sci. Rep.*, vol. 11, Apr. 2021.

[10] G. Soldi, N. Forti, D. Gaglione, P. Braca, L. M. Millefiori, S. Marano, P. Willett, and K. Pattipati, "Quickest detection and forecast of pandemic outbreaks: Analysis of COVID-19 waves," *IEEE Commun. Mag.*, Jul. 2021. [Online]. Available: https://arxiv.org/abs/2101.04620

[11] D. Gaglione, P. Braca, L. M. Millefiori, G. Soldi, N. Forti, S. Marano, P. Willett, and K. R. Pattipati, "Adaptive Bayesian learning and forecasting of epidemic evolution - Data analysis of the COVID-19 outbreak," *IEEE Access*, vol. 8, pp. 175 244–175 264, Sep. 2020.

[12] H. V. Poor, *An Introduction to Signal Detection and Estimation*. Berlin Heidelberg, Germany: Springer-Verlag, 1988.

[13] S. M. Kay, *Fundamentals of Statistical Signal Processing, Volume II: Detection Theory*. Upper Saddle River, NJ, USA: Prentice Hall, 1998.

[14] M. Basseville and I. Nikiforov, *Detection of Abrupt Changes: Theory and Application*. Upper Saddle River, NJ, USA: Prentice Hall, 1993.

[15] A. Tartakovsky, I. Nikiforov, and M. Basseville, *Sequential Analysis: Hypothesis Testing and Changepoint Detection*. Boca Radon, FL, USA: CRC Press, 2014.

[16] Italian Civil Protection Department, "COVID-19 data Italy," https://github.com/pcm-dpc/COVID-19/, 2020.